DE-FG22-94PC94207--14

DOE/PC/94207--14

# High Temperature Electrochemical Polishing of $H_2S$ From Coal Gasification Process Streams

## Quarterly Report
## October 1 - December 31, 1997

**By:**
**Jack Winnick**

Work Performed Under Contract No.: DE-FG22-94PC94207

For
U.S. Department of Energy
Office of Fossil Energy
Federal Energy Technology Center
P.O. Box 880
Morgantown, West Virginia 26507-0880

By
Georgia Institute of Technology
School of Chemical Engineering
Atlanta, Georgia 30332-0100

# DISCLAIMER

## Abstract

An advanced process for the separation of hydrogen sulfide from coal gasification streams through an electrochemical membrane is being perfected. $H_2S$ is removed from a synthetic gas stream, split into hydrogen, which enriches the exiting syn-gas, and sulfur, which is condensed downstream from an inert sweep gas stream. The process allows for continuous removal of $H_2S$ without cooling the gas stream while allowing negligible pressure loss through the separator. Moreover, the process is economically attractive due to the elimination of the need for a Claus process for sulfur recovery. To this extent the project presents a novel concept for improving utilization of coal for more efficient power generation.

## Table of Contents

# Executive Summary

This quarter's research primarily focused on fabricating $LiCoO_2$ electrodes suitable for utilization as the cathode in full cell experimental runs. Appropriate sintering conditions have been established. However, electrode porosity and pore size distribution will need to be improved in order for this material to be successful as the cathode. The primary variables that were studied included: initial concentration of poreformer, initial concentration of binder, initial $LiCoO_2$ particle size, dry pressing times, and pressures. SEM, X-ray diffraction, and particle size analysis were three techniques that were employed to help characterize the fabrication process. Fabricated $LiCoO_2$ electrodes were utilized in full cell experiments at 650 °C. The system successfully transported $CO_3^{2-}$, as expected, with clean fuel gas, and also transported $H_2S$ from contaminated gas. However, the cathode showed inefficient porosity to tallow mass transfer of the extremely dilute $H_2S$ to the electrolyte interface. Thus, $H_2S$ removal efficiencies were below theoretical. However, the electrodes did show the expected high electronic conductivity needed after equilibrating with the $H_2S$-containing gas.

## Project Objectives

Coal may be used to generate electrical energy by any of several processes, most of which involve combustion or gasification. Combustion in a coal-fired boiler and power generation using a steam-cycle is the conventional conversion method; however total energy conversion efficiencies for this type of process are only slightly over 30%[1]. Integration of a gas-cycle in the process (combined cycle) may increase the total conversion efficiency to 40%[1]. Conversion processes based on gasification offer efficiencies above 50%[1].

$H_2S$ is the predominant gaseous contaminant in raw coal gas. Coal depending on the type and area of extraction can contain up to 5 wt% sulfur, which is converted to gaseous $H_2S$ during gasification. Problems arise due to the corrosive nature of $H_2S$ on metal components contained in these cycles. Because of this, $H_2S$ concentrations must be reduced to low levels corresponding to certain power applications. For example, an integrated coal gasification-combined cycle (IGCC) process producing electricity from coal at nearly 50% overall efficiency[1] incorporates gas turbines that cannot tolerate $H_2S$ levels above 100 ppm. Coal gasification/Molten Carbonate Fuel-Cell(MCFC) systems, achieving conversion efficiencies around 60%[2], function properly only if $H_2S$ is below 1 ppm.

An advanced process for the separation of hydrogen sulfide ($H_2S$) from coal gasification product streams through an electrochemical membrane is being developed using funds from this grant. $H_2S$ is removed from the syn-gas stream, split into hydrogen, which enriches the exiting syn-gas, and sulfur, which is condensed from an inert sweep gas stream, Figure 1. The process allows removal of $H_2S$ without cooling the gas stream and with negligible pressure loss through the separator. The process is made economically attractive by the lack of need for a Claus process for sulfur recovery. To this extent the project presents a novel concept for improving utilization of coal for more efficient power generation.

Past experiments using this concept dealt with identifying removal of 1-2% $H_2S$ from gases containing only $H_2S$ in $N_2$[3], simulated natural gas[4,5], and simulated coal gas[6]. Data obtained from these experiments resulted in extended studies into electrode kinetics and electrode stability in molten melts[7,8,9]. The most recent experiments evaluated the polishing application (removal of $H_2S$ below 10 ppm) using the Electrochemical Membrane Separator (EMS). $H_2S$ removal efficiencies over 90% were achieved at these stringent conditions of low $H_2S$ concentrations proving the technologies polishing capabilities.

Other goals include optimization of cell materials capable of improving cell performance. Once cell materials are defined, cell experiments determining maximum removal capabilities and current efficiencies will be conducted.

Also, a model theoretically describing the preferred reduction of $H_2S$, the transport of $S^{2-}$, and the competing transport of $CO_2$ will be investigated. The model should identify the maximum current efficiency for $H_2S$ removal, depending on variables such as flow rate, temperature, current application, and the total cell potential.

## Introduction

The Electrochemical Membrane Separator (E.M.S.), the focus of experimental work, purges a fuel gas contaminated with $H_2S$. This is done by reducing the most electro-active species in the gas stream. In this case, $H_2S$ is reduced by the following:

$$H_2S + 2e^- \rightarrow H_2 + S^{2-} \qquad (1)$$

A membrane which contains sulfide ions in a molten salt electrolyte will act to transport the ions across to the anode. If the membrane is impermeable to $H_2$ diffusion from the cathode side, an inert sweep gas can be used to carry the vaporous oxidized sulfur downstream to be condensed.

$$S^{2-} \rightarrow 1/2\ S_2 + 2e^- \qquad (2)$$

Processes to remove $H_2S$ typically rely on low to ambient temperature adsorption, followed by sorbent regeneration and Claus plant treatment for conversion of $H_2S$ to a salable by-product, sulfur. Although effective, this type of removal is very process-intensive as well as energy-inefficient due to low temperature operation. Gasification streams generally range from 500°C - 1000°C, requiring cooling before and reheating after process gas sweetening. Although these technologies have proven capable of meeting $H_2S$ levels required by MCFC, there are several disadvantages inherent to these processes[10,11].

Alternative high temperature methods are presently available, but process drawbacks including morphological changes in catalytic beds[12] or inefficient molten salt sorbent processes[13] negate savings incurred through energy efficient removal temperatures.

An electrochemical membrane separation system for removing $H_2S$ from coal gasification product streams is the subject of this investigation. The high operating temperature, flow-through design, and capability of selective $H_2S$ removal and direct production of elemental sulfur offered by this process provide several advantages over existing and developmental $H_2S$ removal technologies.

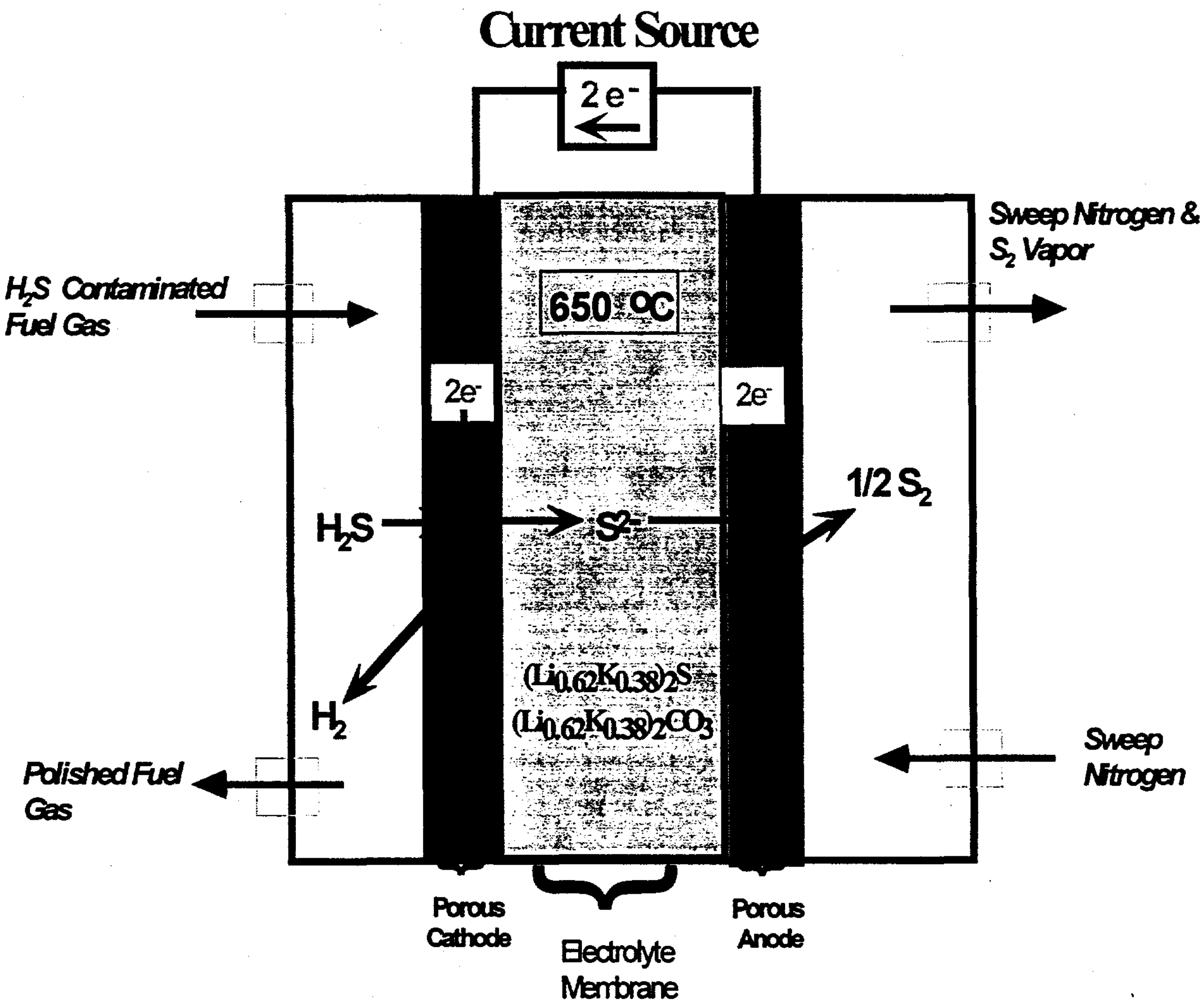

Figure 1. Single-Cell View of the Electrochemical Membrane Separator

## Results and Discussion

A majority of this quarter was spent fabricating $LiCoO_2$ electrodes. One of these electrodes was utilized in a full cell run. Beforehand, one electrode was subjected to sulfurizing conditions in a molten carbonate environment to study the conversion of the $LiCoO_2$ electrode to its sulfided state. In addition, one full cell run was attempted with stainless steel cell housings. All of these results will be discussed in detail below.

### $LiCoO_2$ Electrode Fabrication

$LiCoO_2$ was produced from the calcination reaction of $CoCO_3$ and $Li_2CO_3$ at 700 °C. The $LiCoO_2$ powder was then properly identified by X-ray diffraction and was ready for future use. Dry pressing proved to be the most feasible way to fabricate electrodes, thus this method was chosen. Four electrode batches were attempted; conditions are indicated in Tables 1 - 4. For all electrode fabrication attempts, the hydraulic ram pressure and sintering conditions were consistent. Disks were pressed at 11500 psi for approximately 10 minutes. The sintering program is as follows: ramp of 1°C/min to 500°C for 4 hours, ramp of 1°C/min to 850°C for five hours, ramp of 2°C/min to room temperature. The diameter of the die was 1.25" in all cases.

The first batch, shown in Table 1, had three electrodes with moderate (75%) amounts of $LiCoO_2$ and three electrodes with extremely high (95%) amounts of $LiCoO_2$. It is obvious from the resulting porosities that there must be significant amounts of binder and poreformer to fabricate an adequate electrode. Disks pressed with 95% $LiCoO_2$ resulted in less than 35% porosity. Higher porosities (66%) were observed when 25% poreformer was combined with 75% $LiCoO_2$. Upon sintering, however, the resulting disk crumbled to the touch and was

## Table 1. Conditions for $LiCoO_2$ Electrode Fabrication, Batch #1

| Electrode # | Composition | Weight before sintering (g) | Weight after sintering (g) | Area ($cm^2$) | Thick-ness (cm) | Porosity (%) | Sintering Plate Code |
|---|---|---|---|---|---|---|---|
| 1 | 1% MC<br>4% PF<br>95% $LiCoO_2$ | 1.518 | 1.350 | 5.31 | 0.074 | 32 | 5 |
| 2 | 1% MC<br>4% PF<br>95% $LiCoO_2$ | 1.508 | 1.285 | N/A | N/A | N/A | 5 |
| 3 | 25 % PF<br>75% $LiCoO_2$ | 1.257 | 0.664 | 4.45 | 0.086 | 66 | 5 |
| 4 | 1% MC<br>4% PF<br>95% $LiCoO_2$ | 1.300 | 1.252 | 5.35 | 0.071 | 35 | 3 |
| 5 | 25% MC<br>75% $LiCoO_2$ | 1.417 | 1.003 | 4.83 | 0.075 | 45 | 3 |
| 6 | 25% MC<br>75% $LiCoO_2$ | 1.400 | 0.983 | 4.52 | 0.100 | 57 | 2 |

Notes: MC = Methyl cellulose PF = Carbon poreformer

Plate Codes:

2 = 5 cm diameter alumina disk
3 = 2.5" x 2.5" thin alumina plate
5 = 5" diameter alumina plate

Table 2. Conditions for $LiCoO_2$ Electrode Fabrication, Batch #2

| Electrode # | Composition | Weight before sintering (g) | Weight after sintering (g) | Area ($cm^2$) | Thick-ness (cm) | Porosity (%) |
|---|---|---|---|---|---|---|
| 1 | 15% MC<br>10% PF<br>75% $LiCoO_2$ | 1.551 | N/A | N/A | N/A | N/A |
| 2 | 15% MC<br>10% PF<br>75% $LiCoO_2$ | 1.488 | N/A | N/A | N/A | N/A |
| 3 | 15% MC<br>15% PF<br>70% $LiCoO_2$ | 1.525 | N/A | N/A | N/A | N/A |
| 4 | 15% MC<br>15% PF<br>70% $LiCoO_2$ | 1.562 | N/A | N/A | N/A | N/A |
| 5 | 20% MC<br>10% PF<br>70% $LiCoO_2$ | 1.662 | N/A | N/A | N/A | N/A |
| 6 | 20% MC<br>10% PF<br>70% $LiCoO_2$ | 1.468 | N/A | N/A | N/A | N/A |
| 7 | 20% MC<br>5% PF<br>75% $LiCoO_2$ | 1.5 | N/A | N/A | N/A | N/A |

Notes: Electrodes failed upon sintering (none were in disk form).

**Table 3. Conditions for $LiCoO_2$ Electrode Fabrication, Batch #3**

| Electrode # | Composition | Weight before sintering (g) | Weight after sintering (g) | Area ($cm^2$) | Thick-ness (cm) | Porosity (%) | Sintering Plate Code |
|---|---|---|---|---|---|---|---|
| 1 | 15% MC<br>5% PF<br>80% $LiCoO_2$<br>(μ=2 μm) | 1.463 | 1.041 | 5.853 | 0.108 | 67 | 1 |
| 2 | 15% MC<br>5% PF<br>80% $LiCoO_2$<br>(μ=2 μm) | 1.486 | 1.139 | 5.228 | 0.085 | 49 | 2 |
| 3 | 15% MC<br>5% PF<br>80% $LiCoO_2$<br>(μ=14 μm) | 1.493 | 1.109 | 5.147 | 0.072 | 41 | 3 |
| 4 | 15% MC<br>5% PF<br>80% $LiCoO_2$<br>(μ=14 μm) | 1.480 | 1.166 | 5.067 | 0.085 | 46 | 4 |
| 5 | 15% PVA<br>5% PF<br>80% $LiCoO_2$<br>(μ=14μm) | 1.425 | 1.072 | 4.909 | 0.081 | 47 | 3 |
| 6 | 15% PVA<br>5% PF<br>80% $LiCoO_2$<br>(μ=14μm) | 1.518 | 1.123 | 4.988 | 0.084 | 47 | 4 |

Notes: MC = Methyl Cellulose PVA = Polyvinyl alcohol PF = Carbon poreformer

Plate Codes:

1 = 3" x 3" porous cell housings
2 = 5 cm diameter alumina disk
3 = 2.5" x 2.5" thin alumina plate
4 = 3" diameter ceramic disk

**Table 4. Conditions for $LiCoO_2$ Electrode Fabrication, Batch #4**

| Electrode # | Composition | Weight before sintering (g) | Weight after sintering (g) | Area ($cm^2$) | Thick-ness (cm) | Porosity (%) | Sintering Plate Code |
|---|---|---|---|---|---|---|---|
| 1 | 20% MC<br>10% PF<br>70% $LiCoO_2$<br>($\mu$=4.29 $\mu$m) | 1.432 | 0.945 | N/A | N/A | N/A | 3 |
| 2 | 20% MC<br>10% PF<br>70% $LiCoO_2$<br>($\mu$=4.29 $\mu$m) | 1.503 | 0.974 | 4.87 | 0.109 | 64 | 2 |
| 3 | 17% MC<br>8% PF<br>75% $LiCoO_2$<br>($\mu$=4.29 $\mu$m) | 1.530 | 1.068 | 4.99 | 0.093 | 54 | 3 on top of 1 |
| 4 | 17% MC<br>8% PF<br>75% $LiCoO_2$<br>($\mu$=4.29 $\mu$m) | 1.459 | 1.061 | 4.91 | 0.095 | 55 | 2 |

Notes: MC = Methyl cellulose PF = Carbon poreformer

Plate Codes:

1 = 3" x 3" porous cell housings
2 = 5 cm diameter alumina disk
3 = 2.5" x 2.5" thin alumina plate
4 = 3" diameter ceramic disk

cracked in half. Disks pressed with only 25% methyl cellulose and 75% $LiCoO_2$ resulted in compact disks after sintering, but porosities were too low (45% and 57%). SEM of Electrode #6, which contained 25% methyl cellulose, revealed pore sizes on the order of 10 microns. A photograph of this electrode is shown in Figure 2. This photograph shows that adequate porosity was achieved, but increased porosity is desired. Therefore, it was concluded that the next batch should have a significant amount of binder and poreformer.

The second batch, shown in Table 2, tried to address the problems which were discovered in the first batch. Three different initial concentrations were attempted - 15% methyl cellulose, 10% poreformer; 15% binder, 15% poreformer; and 20% binder, 10% poreformer. Upon sintering, all disks failed (powder was spread throughout with no cohesiveness). Before this batch, the particle size of $LiCoO_2$ had not been measured. It was determined that the failure of the second batch may have been due to the large particle size of the $LiCoO_2$. Particle size analysis revealed that the 50% median particle size was 22 microns. To achieve proper disk strength, particle size distribution, and porosity, initial $LiCoO_2$ particle size needs to be smaller. Therefore, samples of $LiCoO_2$ were ball milled for 24 - 36 hours for future sintering experiments.

The third sintering batch (Table 3) had binder and poreformer concentrations similar to the second batch, but the particle size of $LiCoO_2$ was reduced. Four disks had 15% methyl cellulose, 5% carbon poreformer, and 80% $LiCoO_2$, with two of these disks having an $\mu_{50\%}$ of 14 microns and the other two with $\mu_{50\%}$ of 2 microns. The resulting sintered disks all appeared solid. The two disks with the smaller initial particle size (2 microns) had much larger porosities (67% and 49%) compared with the larger initial particle size (14 microns), whose porosities were 41% and 46%. Two other disks were attempted - with 15% polyvinyl alcohol and 5% poreformer.

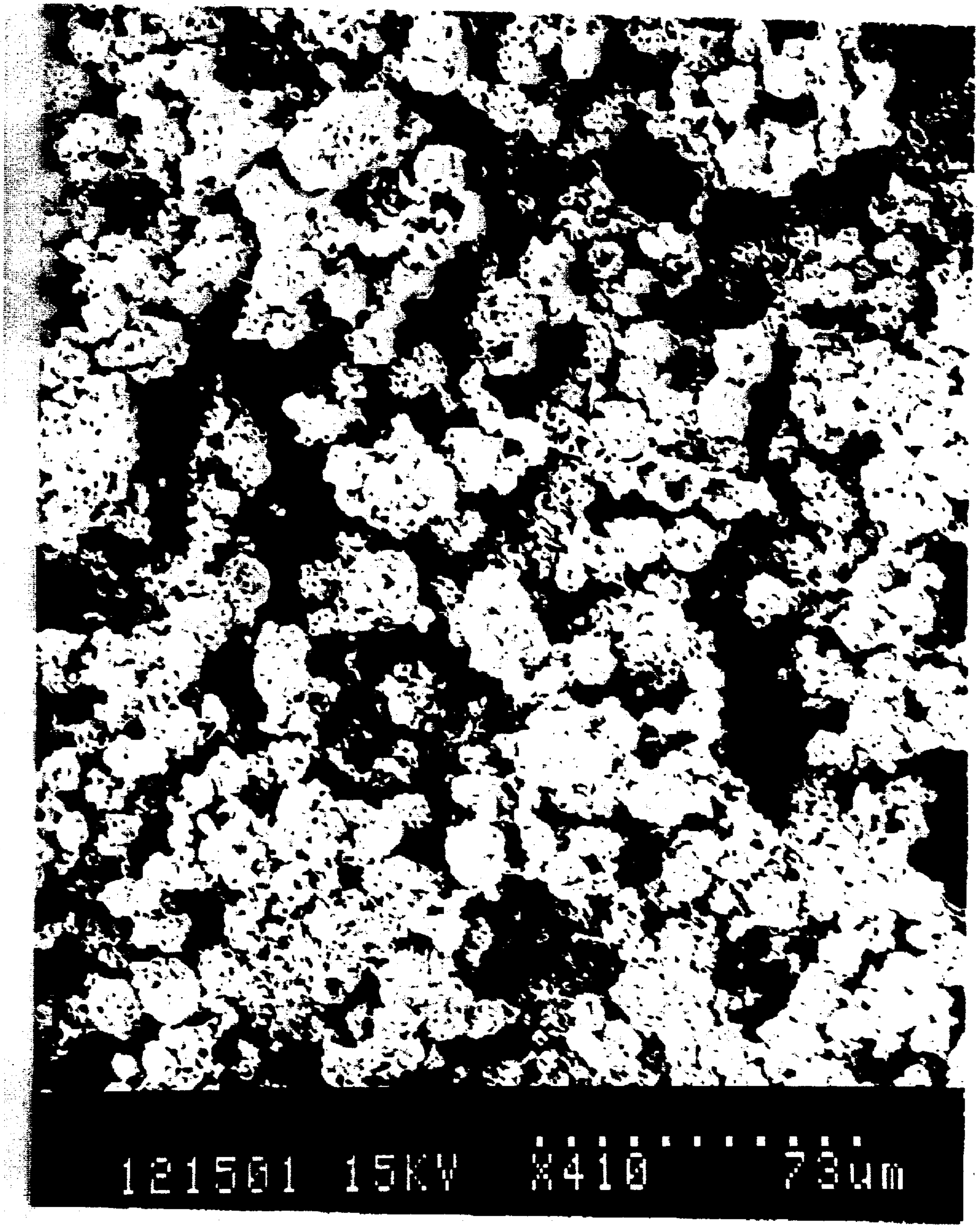

1-91 #6

Figure 2. SEM of Electrode #6, Batch #1: Porosity = 57%

The resulting sintered disks were cohesive, but not qualitatively as good as the other four. Slight cracks and non-circular shapes plagued the two disks. Resulting porosities were 47% for both disks. This batch led us to conclude that smaller $LiCoO_2$ particle size was important in a resulting sintered disk's strength and porosity. The success of methyl cellulose over polyvinyl alcohol dictated that methyl cellulose be the designated binder in future sintering experiments.

The fourth batch of $LiCoO_2$ electrodes this quarter (see Table 4) consisted of four pressed disks. In order to increase porosity, the poreformer and binder concentrations were increased. Two electrodes had 20% methyl cellulose, 10% carbon poreformer, and 70% $LiCoO_2$ while the other two electrodes consisted of 17% methyl cellulose, 8% carbon poreformer, and 25% $LiCoO_2$. The resulting electrodes were more porous, with porosities ranging from 55 to 64%. Progression is being made in $LiCoO_2$ electrode fabrication. Further work in this area will attempt to increase electrode porosity even further without sacrificing electrode strength and durability.

## $LiCoO_2$ electrode test in sulfurizing and molten carbonate conditions

A fabricated $LiCoO_2$ (from Batch #1, Electrode #4, 35% porosity) disk was subject to a cell run which mimicked the conditions that it would encounter as the cathode in a full cell run. A MACOR ceramic housing was utilized to hold the disk in place. Gold wires running through alumina tubes connected to the MACOR cell housing terminated at the $LiCoO_2$ disk to measure the conductivity of the material. A Zircona membrane which was impregnated with $(Li_{0.68}K_{0.32})_2CO_3$ was placed on top of the $LiCoO_2$-containing MACOR cell housing. A 3" diameter alumina plate was placed on top of this and a 1.6 kg weight was added to ensure no gas leakage. This apparatus was placed in a furnace and the temperature was gradually increased to

650 °C. Then, process gases were introduced to one of the alumina tubes. The inlet gas concentrations were approximately: 7.7% $H_2O$, 3.6% $CO_2$, 1.1% CO, 5.0 % $H_2$, 3000 ppm $H_2S$, and balance $N_2$. The $LiCoO_2$ was subject to these conditions for 50 hours. X-ray diffraction (see Figure 3) of the resulting sample revealed peaks for $Co_3S_4$, $Co_4S_3$, and $Co_9S_8$, which are highly conductive compounds. A crude conductivity analysis demonstrated that the conductivity fell from over 100 ohms at the beginning of the experiment to less than 2 ohms at the end when the electrode had been totally sulfided. These results lead us to believe that $LiCoO_2$ can be utilized as a successful cathode material if the pore size and porosity are manipulated correctly.

### Full-Cell Experimental Run with a $LiCoO_2$ Cathode

There were two attempts at full cell $H_2S$ removal experiments this quarter utilizing $LiCoO_2$ as the cathode. Run #45 was plagued by connection problems between the current collector and the cathode. The cathode, which was in the top cell housing, was too thin and did not have proper contact between the membrane and the gold current collector. Therefore, this run was terminated before any data collection. Run #46 attempted to alleviate the contact problem by placing the $LiCoO_2$ cathode in the bottom cell housing and the nickel anode in the top cell housing. Initially, however, there were still cathode-current collector-membrane contact problems. Therefore, the cell was cooled to room temperature. Then, additional and thicker gold current collector was added inside the cell housings. Also, the $LiCoO_2$ cathode and Zircar membrane, which cracked upon cooldown, were replaced. Table 5 summarizes the conditions for the two full-cell runs.

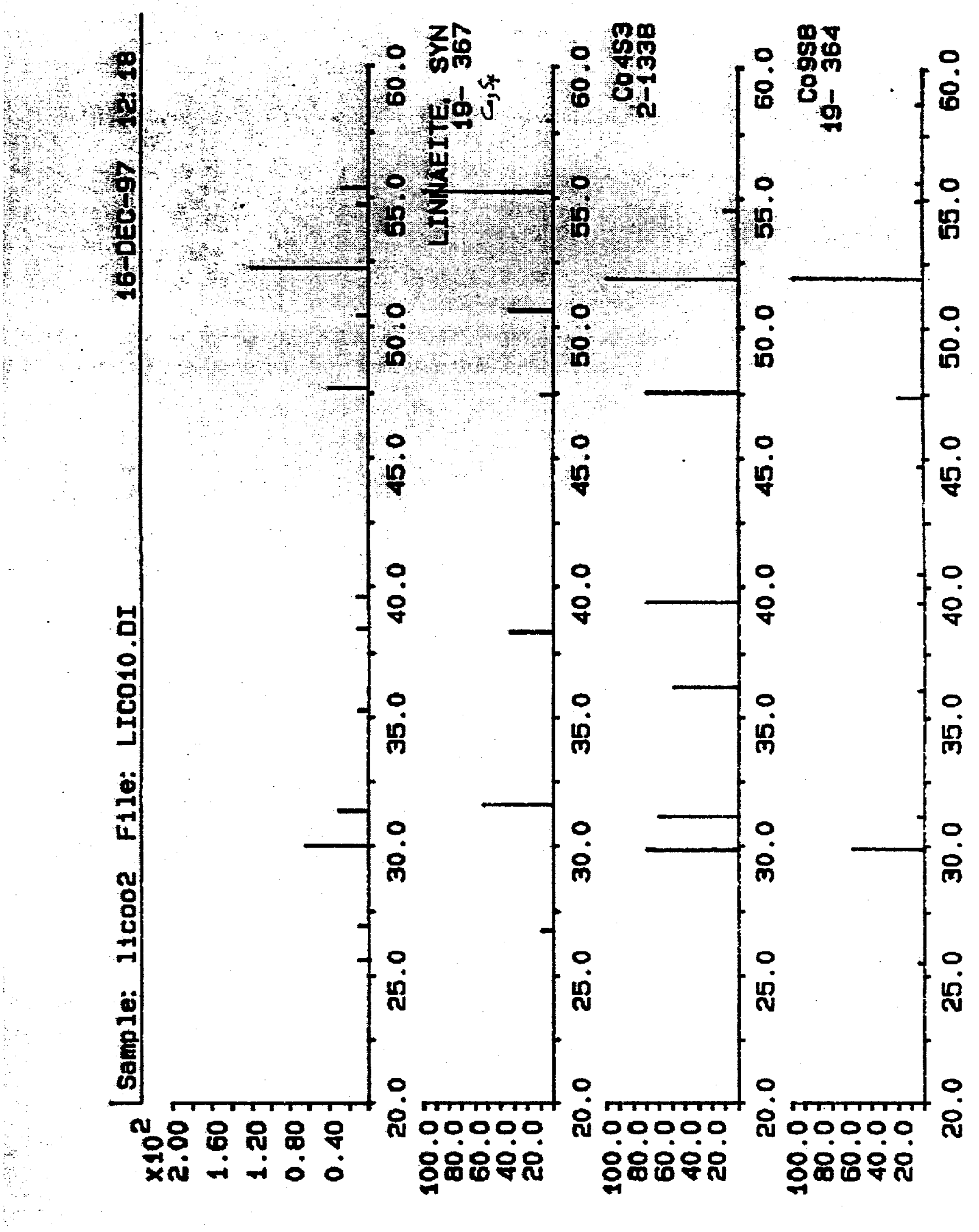

Figure 3. $LiCoO_2$ after 50 hours in sulfurizing conditions.

**Table 5. Full Cell Runs with $LiCoO_2$ Cathodes Attempted this Quarter**

| Run # | Temp ( °C) | Cathode | Anode | Membrane | Housings | Passivation |
|---|---|---|---|---|---|---|
| 45 | 650 | $LiCoO_2$<br>Batch#4,#3<br>55%porosity | Lithiated Ni | Fabricated $ZrO_2$ | MACOR | None |
| 46 | 650 | $LiCoO_2$<br>Batch#4,#3<br>54%porosity<br>&<br>$LiCoO_2$<br>Batch#3,#4<br>46%porosity | Lithiated Ni | Fabricated $ZrO_2$ | MACOR | None |

Carbonate Transport

Before the addition of $H_2S$ to the cell, it is necessary to evaluate the electrochemical membrane separator's ability to transport carbonate across the cell. This is accomplished by $CO_2$ removal from the process gas (cathode coal syn-gas) (**3**):

$$CO_2 + H_2O + 2e^- -> H_2 + CO_3^{2-} \tag{3}$$

and anode $CO_2$ evolution due to carbonate oxidation (**4**):

$$CO_3^{2-} -> CO_2 + \frac{1}{2}O_2 + 2e^- \tag{4}$$

This is the first test performed during a full-cell run which displays the EMS cell's performance. Based on 2 Faraday's of charge transferred per mole of species reduced or oxidized, the actual carbon dioxide removed/produced can be compared to theoretical amounts. A current step method is utilized to determine the carbon dioxide removal, carbon dioxide production, as well as cell potential at varying applied currents. Due to a faulty IR analyzer, $CO_3^{2-}$ transport data was not taken at this stage of the experiment. However, the machine was fixed and used to measure anode $CO_2$ levels during $H_2S$ removal experiments.

## Removal of $H_2S$ from Sour Coal Gas

Once carbonate transport across the cell was demonstrated, $H_2S$ was added to the process syn-gas. The process gas was equilibrated by the following two reactions:

$$\mathbf{H_2 + CO_2 \Leftrightarrow H_2O + CO} \tag{5}$$

$$\mathbf{H_2S + CO \Leftrightarrow H_2 + COS} \tag{6}$$

via a stainless steel shift reactor before entering the cell housing. Once process gases entered the cell housings, they equilibrated with the molten electrolyte by:

$$\mathbf{(Li_{0.68}K_{0.32})_2CO_3 + H_2S \Leftrightarrow (Li_{0.68}K_{0.32})_2S + CO_2 + H_2O} \tag{7}$$

which creates a conversion of carbonate ions to sulfide ions depending on the concentration of $H_2S$ in contact with the electrolyte as well as the temperature of the cell. Increased temperatures result in higher molten sulfide concentrations which facilitate sulfide oxidation. Typically, at least twenty-four hours is necessary for this reaction to reach equilibrium.

The goal of full-cell experiments is to validate the removal capabilities of the EMS system while maintaining economically feasible current efficiencies (high current efficiencies at high inlet $H_2S$ concentrations). $H_2S$ current efficiency is calculated by:

$$\eta_{H_2S} = \frac{\mathbf{\%\,H_2S\ Removal_{actual}}}{\mathbf{\%\,H_2S\ Removal_{theoretical}}} \tag{8}$$

which represents the ratio of $H_2S$ actually removed to the amount that should be removed at a specified applied current. The following equation calculates the amount of $H_2S$ removed from the process syn-gas:

$$\%\ \mathbf{H_2S\,Removal} = \frac{\mathbf{Inlet\ H_2S - Outlet\ H_2S_{(I_{app})}}}{\mathbf{Inlet\ H_2S}}\ \mathbf{x100} \qquad \mathbf{(9)}$$

Run #46 was tested for $H_2S$ removal at two flow rates for $H_2S$ inlet values around 2500 ppm, which will be subtitled Run #46a and #46b. Both runs occurred at 650 °C. Run #46a had a cathode inlet flow rate of 181 cc/min, with a corresponding outlet flow of 90 cc/min. The process gases equilibrated to: 4.9% $CO_2$, 2.20% CO, 7.1% $H_2O$, 7.1% $H_2$, 2500 ppm $H_2S$, and balance $N_2$. The molten salt equilibrium concentration was estimated at 83% $M_2CO_3$ and 17% $M_2S$, where M represents the lithium/potassium eutectic. The gas phase limiting current density was estimated at 29.6 $mA/cm^2$, while the membrane limiting current density was estimated at 170 $mA/cm^2$. With an electrode area of 5.07 $cm^2$, the limiting current density for these conditions was 150 mA. Applied current approaching this level will result in severe mass transfer limitations. Anode inlet and outlet flow rates for this run were approximately 208 and 109 cc/min, respectively.

Run #46b had an increased cathode flow rate of 297 cc/min with an inlet $H_2S$ concentration of 2200 ppm. The cathode inlet gas was estimated as follows: 4.35% $CO_2$, 1.65% CO, 7.34% $H_2O$, 6.20% $H_2$, 2200 ppm $H_2S$, and balance $N_2$. Limiting current densities in the gas phase and membrane were estimated at 26.1 and 166 $mA/cm^2$, respectively. Molten salt equilibrium was estimated at 84.3% $M_2CO_3$ and 15.7% $M_2S$.

A current step was applied to determine the $H_2S$ outlet levels, %$H_2S$ removal, current efficiency, and the electrode overpotentials. Figure 4 demonstrates that $H_2S$ outlet levels fall with increasing cell current for the two different flow rates. Figure 5 shows $H_2S$ removal as a function of applied current. $H_2S$ removal was observed at both flow rates for this run. However,

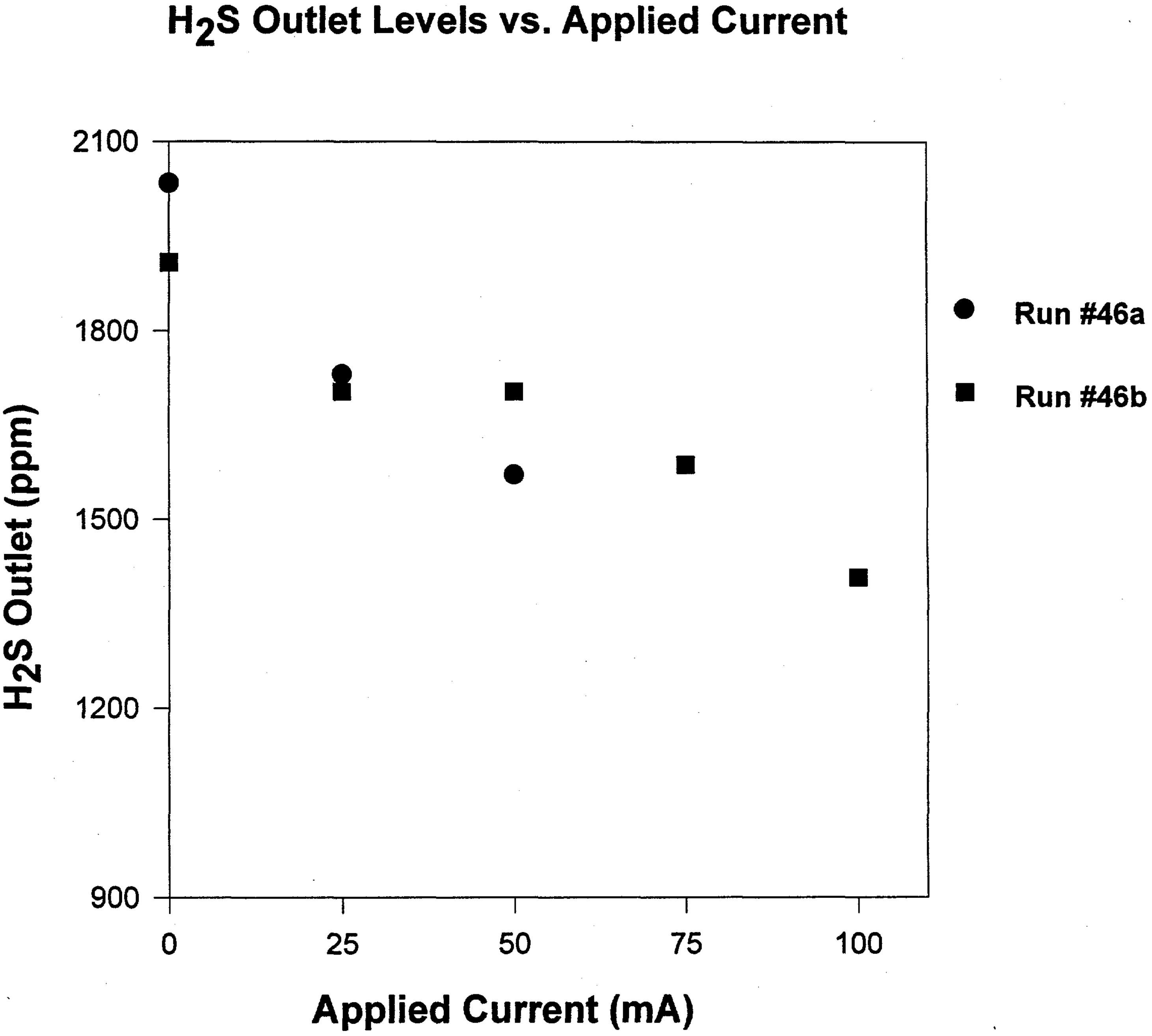

Figure 4. Run #46. $H_2S$ Outlet Levels vs. Applied Current

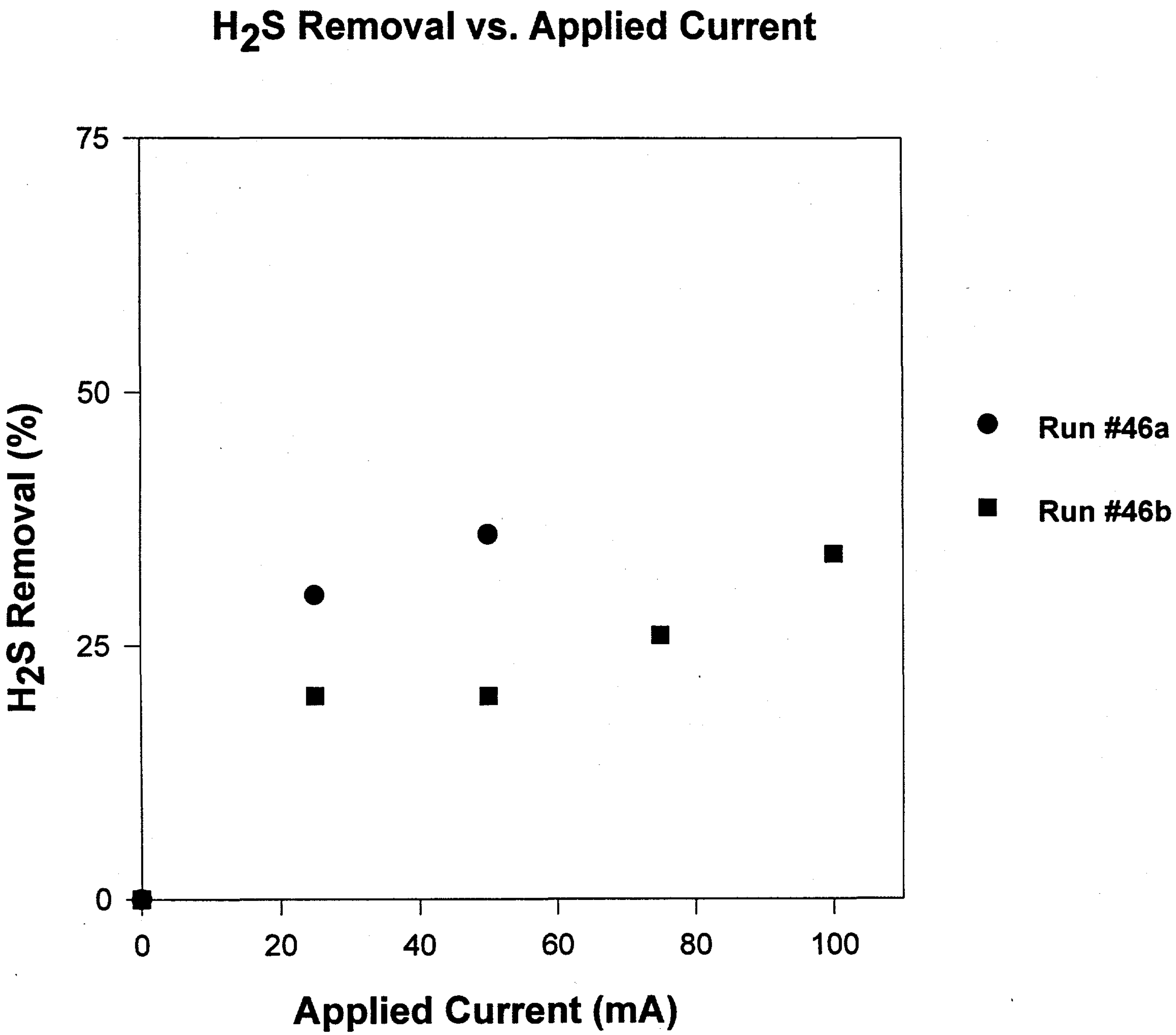

Figure 5. Run #46. $H_2S$ Removal vs. Applied Current

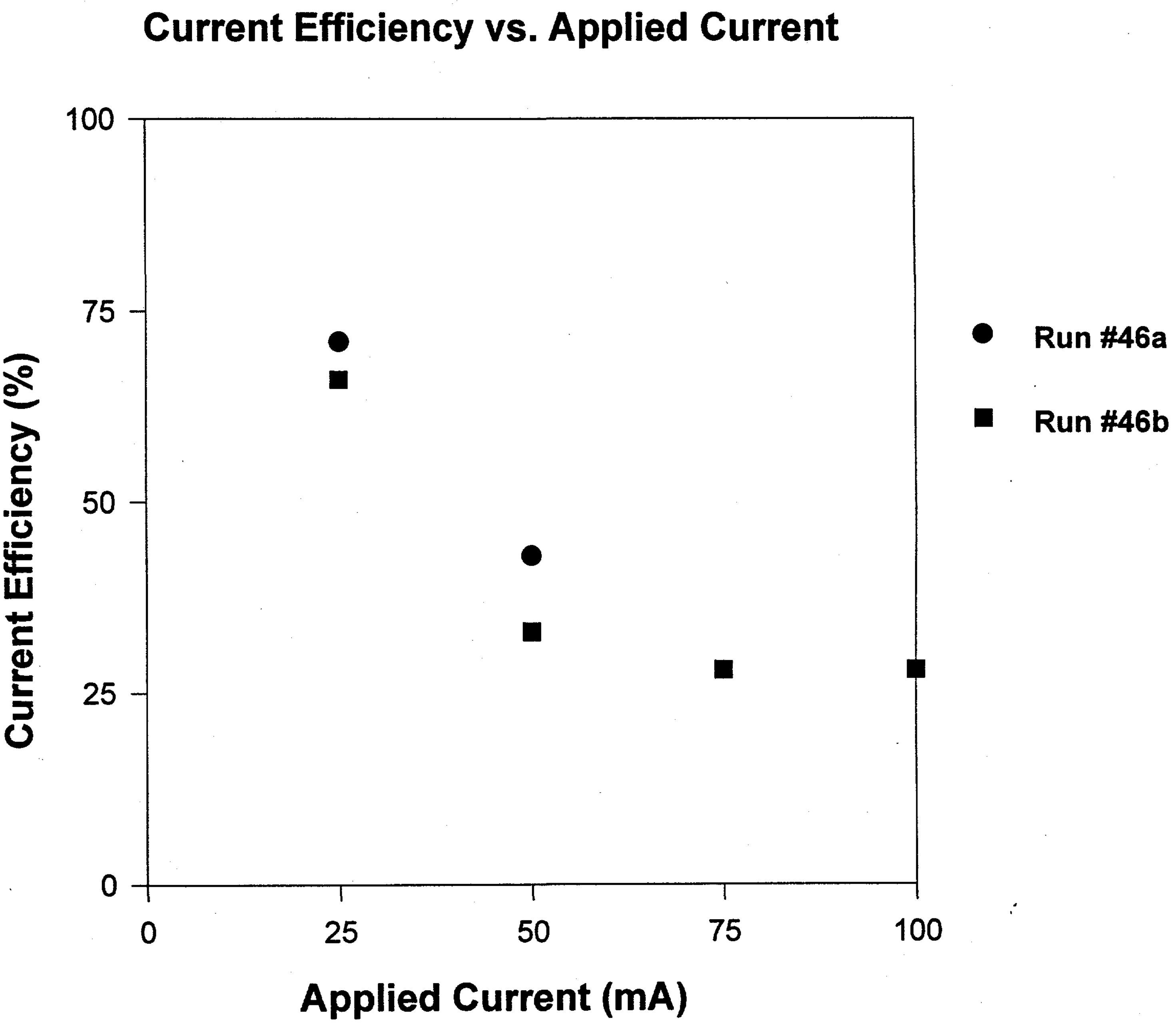

Figure 6. Run #46. Current Efficiency vs. Applied Current

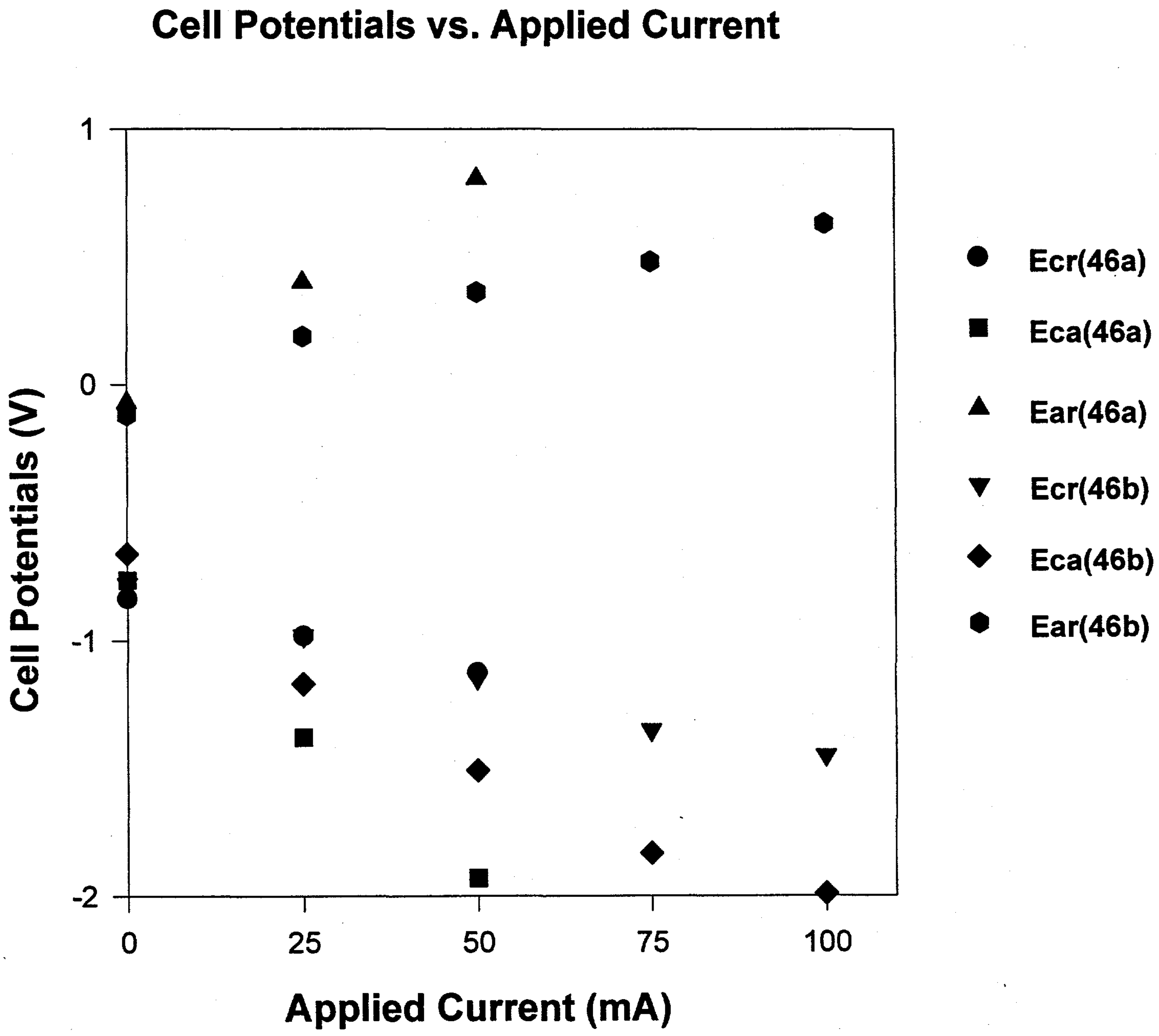

Figure 7. Run #46. Cell Potentials vs. Applied Current

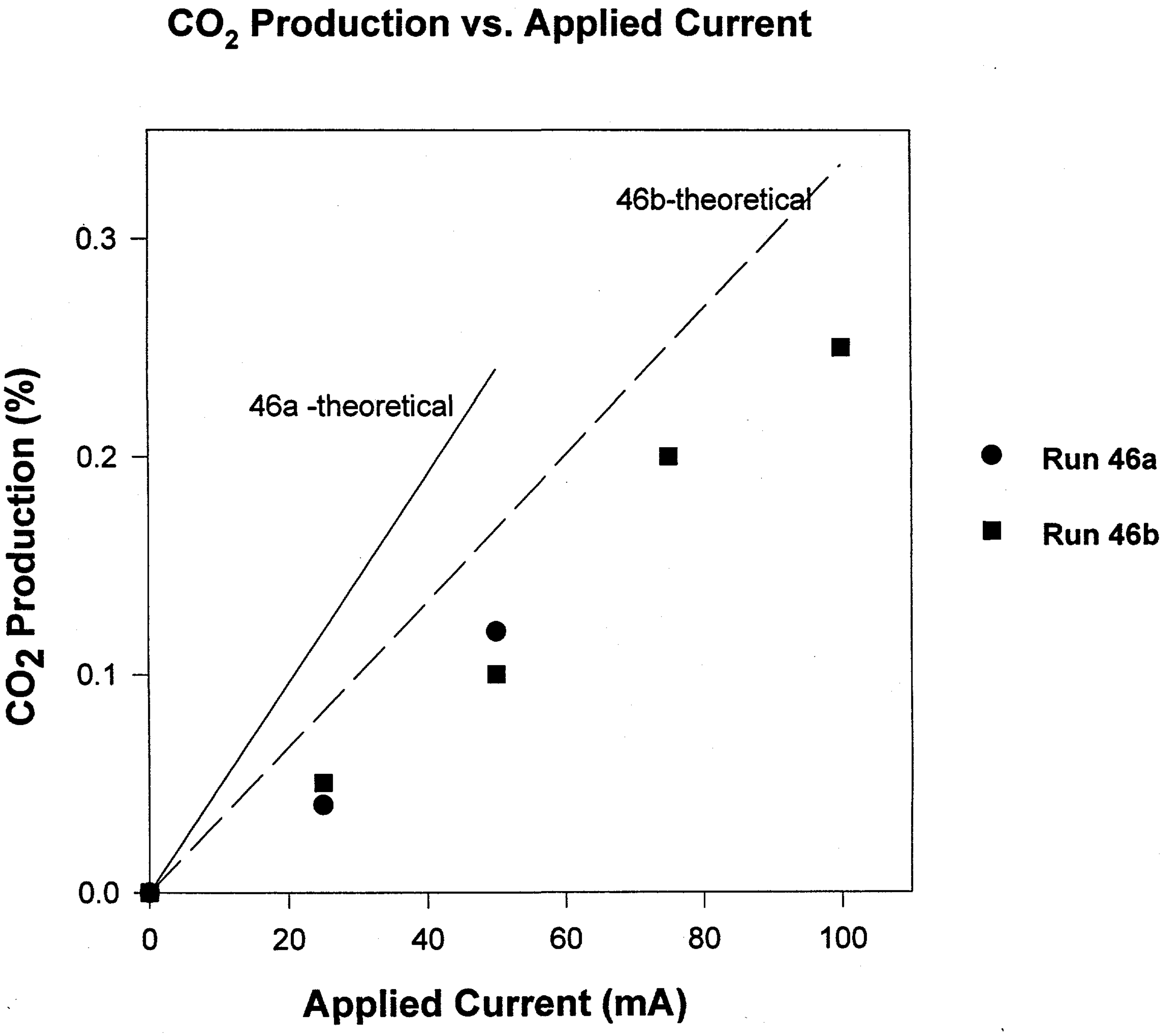

**Figure 8. Run#46. $CO_2$ Production vs. Applied Current**

the $H_2S$ removal was not stoichiometric. Figure 6 illustrates this by showing the decreasing relationship between $H_2S$ current efficiency and applied current. Figure 7 compares cell potentials with applied current. Overpotentials are within reasonable bounds. Ohmic resistance for this entire run was unreasonably high; this was probably due to poor contact between the anode current collector, nickel anode, and electrolyte-filled membrane. The linear relation of the anode-reference potential with applied current implies that there is significant ohmic loss here. Figure 8 shows that $CO_2$ is produced at the anode with increasing applied current. This is a certain sign that carbonate transport is occurring rather than desired sulfide transport. The lack of porosity in the cathode limits the amount of surface area available for reduction. Since $H_2O$ and $CO_2$ are much more abundant than $H_2S$, they will be preferred for reduction when the reaction is mass transfer limited. This results in $CO_3^{2-}$ formation, which is consequently oxidized at the anode to form $CO_2$. The run was eventually stopped after 11 days due to cathode failure (as observed from cathode-reference potentials and lack of $H_2S$ removal). Figure 9 is an SEM photograph of the $LiCoO_2$ electrode after the full cell run.

$LiCoO_2$ was successful as the cathode at removing 2500 ppm $H_2S$ at two different flow rates. While desired removal levels were not achieved, it is presumed that this is purely a lack of electrode optimization. The $LiCoO_2$ cathode porosity of 46% needs to be increased. The highly porous (~90%) nickel electrodes from ERC which have been successfully used in the past at 580°C provide ample pores and surface area to allow for $H_2S$ diffusion from the bulk phase into the electrode where it is then reduced at the electrode/electrolyte interface. $LiCoO_2$ is preferred over nickel since it can operate at a temperature of 650°C, well above the operating range of nickel. However, ultimate success of the $LiCoO_2$ electrode can only be achieved with a higher porosity and proper pore size distribution.

Figure 9. Run #42. SEM Photograph of cathode after experiment.

Full Cell Run with Stainless Steel Cell Housings

One full cell run was attempted this quarter with stainless steel cell housings. The conditions for the run are in the following table:

**Table 6. Full Cell Run Conditions for Experiment #44**

| Run # | Temp (°C) | Cathode | Anode | Membrane | Housings | Passivation |
|---|---|---|---|---|---|---|
| 44 | 580 | Lithiated Ni Thickness: 1.12 mm | Lithiated Ni Thickness: 1.12 mm | Fabricated $ZrO_2$ | Stainless Steel (316) | All areas aluminum passivated |

This experiment also had gold current collectors designed to enhance the contact area between the stainless steel and the electrodes.

Like past experiments with stainless steel cell housings, the EMS was successful at carbonate transport across the cell. Stoichimetric $CO_2$ reduction at the cathode and production at the anode was observed. However, once $H_2S$ is added to the cathode inlet gas mixture, the EMS is plagued by several problems. The primary problem is lack of equilibration between the $H_2S$ cathode inlet and outlet levels. At least three days are typically required for the outlet $H_2S$ values to come within 60% of the inlet values with stainless steel cell housings. For example, in this experiment, the inlet $H_2S$ value was ~2400 ppm. It took four days for the outlet value to reach 1300 ppm. This can be attributed to $H_2S$ adsorption onto stainless steel. Shvartsman and Petrova[14] demonstrated that $H_2S$ adsorption depends on the mean grain size of the metal and the ratio of $P_{H2S}:P_{H2}$ in the gas phase. Our experiment has 8 inch stainless steel tubes leading into and out of the stainless steel cell housing. Therefore, there is abundant stainless steel surface area for $H_2S$ adsorption.

Another interesting observation utilizing stainless steel cell housings should be noted. Previously utilized cell housings that had been subject to $H_2S$ for long periods of time still contained the $H_2S$ on the stainless steel surface. When subject to a cathode inlet containing only $H_2$, $H_2O$, CO, $CO_2$, and $N_2$, the resulting cathode outlet contained at least 400 ppm $H_2S$. It is assumed that $H_2$ in contact with the sulfided stainless steel forms $H_2S$. It is obvious that this occurrence can have detrimental effects for $H_2S$ removal. Any removal that occurs will be offset by the adsorbed $H_2S$ downstream, which will react with $H_2$ to reform $H_2S$. Thus, limited or no removal will be observed at the cathode outlet. One technique to deter this occurrence is a ceramic cathode tube outlet. This will eliminate some potential $H_2S$ adsorption as well as prevent downstream $H_2S$ reformation.

## Conclusion

$LiCoO_2$ has been proven to be a successful alternative to the nickel cathode. In addition, it can operate at 650 °C, which is favorable because this is the common gasifier temperature. Moreover, for our flow conditions, higher temperatures result in higher sulfide concentrations in the molten electrolyte. However, full cell runs employing $LiCoO_2$ as the cathode have been plagued by low current efficiencies. This is due to low cathode porosities, which will hopefully be increased in the near future.

Full cell $H_2S$ removal runs with stainless steel cell housings may be limited by $H_2S$ adsorption onto the cell housings as well as the stainless steel inlet and exit tubes. This has deleterious effects in two ways. First, cathode $H_2S$ outlet levels require long periods of time to reach cathode inlet levels. Second, the adsorbed $H_2S$ reacts with hydrogen in the presence of lower non-equilibrium $H_2S$ levels to reform $H_2S$. Therefore, removal experiments are more difficult to quantify.

## Projected Work

This quarter, full cell runs with alumina ($Al_2O_3$) plasma coated stainless steel cell housings will be performed. The alumina is being plasma coated by Plasma Coatings, Inc., the same company who previously plasma coated aluminum onto the cell housings. The alumina should provide a totally nonconductive layer so that no current is lost to undesired side reactions. The outlet tube from the stainless steel cell housing will be ceramic, which is nonreactive with $H_2S$. Therefore, the detrimental downstream effects of $H_2S$ adsorption can be avoided.

$LiCoO_2$ porosity will be enhanced by increasing the initial concentration of binder and poreformer. This will be accomplished without sacrificing the strength of the resulting electrode. $H_2S$ removal full cell removal runs at 650 °C will be continued with high porosity electrodes. SEM and X-ray diffraction will be utilized to characterize the $LiCoO_2$ electrodes before and after the cell runs.

## References

1. U.S. Dept of Energy, DOE/METC 87/0255, DE87006493, Oct., 1987.
2. Skerret, P.J., "Fuel Cell Update", *Popular Science*, 89-91, 120-1, June, 1993.
3. Lim, H.S. and Winnick, J., *J. Electrochem. Soc.*, **131, 562-8** (1984).
4. Alexander, S., and Winnick, J., *1990 AIChE Annual Meeting*, Chicago, IL., 1990.
5. Alexander, S., and Winnick, J., *Sep'n Sci. and Tech.*, **25**, 2057-72 (1990).

6. Weaver, D., and Winnick, J., *J. Electrochem. Soc.*, **134**, 2451-58 (1987).

7. Weaver, D., and Winnick, J., *J. Electrochem. Soc.*, **138**, 1626-37 (1991).

8. Banks, E., and Winnick, J., *J. Appl. Electrochem.*, **16**, 583-90 (1986).

9. White, K.A., and Winnick, J., *Electrochim. Acta*, **30**, 511-516 (1985).

10. EPRIEM-1333, *Assessment of Sulfur Removal Processes for Advanced Fuel Cell Systems, Final Report,* C.F. Braun and Co., Alhambra, CA, Jan., 1980.

11. Vidt, E.J., DOE/METC DE-AC-21-81MC16220, DE82013942, Westinghouse, Dec., 1981.

12. Focht, G.D. et. al., DOE/MC/121166-2163, DE86016041, July, 1986.

13. Lyke, S.E., DOE/MC/19077-1803, DE8500961, Battelle Pacific Northwestern Laboratories, Jan. 1985.

14. Shvartsman, L.A., and Petrova, E.F., *Russ Metall Metn,* **5**, 177-179 (1984).